LETTER

doi:10.1038/nature11713

Rapid regulation of depression-related behaviours by control of midbrain dopamine neurons

Dipesh Chaudhury[1]*, Jessica J. Walsh[1,2]*, Allyson K. Friedman[1], Barbara Juarez[1,2], Stacy M. Ku[1,2], Ja Wook Koo[2], Deveroux Ferguson[2], Hsing-Chen Tsai[3], Lisa Pomeranz[4], Daniel J. Christoffel[2], Alexander R. Nectow[4], Mats Ekstrand[4], Ana Domingos[4], Michelle S. Mazei-Robison[2], Ezekiell Mouzon[2], Mary Kay Lobo[2], Rachael L. Neve[5], Jeffrey M. Friedman[4], Scott J. Russo[2], Karl Deisseroth[3], Eric J. Nestler[1,2] & Ming-Hu Han[1,2]

Ventral tegmental area (VTA) dopamine neurons in the brain's reward circuit have a crucial role in mediating stress responses[1–4], including determining susceptibility versus resilience to social-stress-induced behavioural abnormalities[5]. VTA dopamine neurons show two *in vivo* patterns of firing: low frequency tonic firing and high frequency phasic firing[6–8]. Phasic firing of the neurons, which is well known to encode reward signals[6,7,9], is upregulated by repeated social-defeat stress, a highly validated mouse model of depression[5,8,10–13]. Surprisingly, this pathophysiological effect is seen in susceptible mice only, with no apparent change in firing rate in resilient individuals[5,8]. However, direct evidence—in real time—linking dopamine neuron phasic firing in promoting the susceptible (depression-like) phenotype is lacking. Here we took advantage of the temporal precision and cell-type and projection-pathway specificity of optogenetics to show that enhanced phasic firing of these neurons mediates susceptibility to social-defeat stress in freely behaving mice. We show that optogenetic induction of phasic, but not tonic, firing in VTA dopamine neurons of mice undergoing a subthreshold social-defeat paradigm rapidly induced a susceptible phenotype as measured by social avoidance and decreased sucrose preference. Optogenetic phasic stimulation of these neurons also quickly induced a susceptible phenotype in previously resilient mice that had been subjected to repeated social-defeat stress. Furthermore, we show differences in projection-pathway specificity in promoting stress susceptibility: phasic activation of VTA neurons projecting to the nucleus accumbens (NAc), but not to the medial prefrontal cortex (mPFC), induced susceptibility to social-defeat stress. Conversely, optogenetic inhibition of the VTA–NAc projection induced resilience, whereas inhibition of the VTA–mPFC projection promoted susceptibility. Overall, these studies reveal novel firing-pattern- and neural-circuit-specific mechanisms of depression.

To selectively target VTA dopamine neurons, we injected a double-floxed (DIO) Cre-dependent adeno-associated virus (AAV) vector expressing channelrhodopsin-2 (ChR2) fused with enhanced yellow fluorescent protein (eYFP) (AAV-DIO-ChR2–eYFP) into the VTA of tyrosine hydroxylase (TH)–Cre transgenic mice[7,14]. We first validated the specificity and efficacy of AAV-DIO-ChR2–eYFP expression in VTA dopamine neurons of TH–Cre mice *in vivo* (Fig. 1a, b). Next, functional validation of ChR2–eYFP expression in VTA dopamine neurons using *in vitro* and *in vivo* electrophysiological recordings confirmed that optogenetic stimulation enables precise temporal control of these neurons (Supplementary Fig. 1a–c) and can be used to mimic the *in vivo* pathophysiological upregulation in phasic firing seen in the social-defeat-stress model of depression[8,12].

To investigate the functional consequence of the increase in phasic firing of VTA dopamine neurons observed after repeated (10-day) social-defeat stress, we examined the effect of optogenetically inducing tonic (0.5-Hz) or phasic (20-Hz) firing (Fig. 1c; 5 spikes for each 10 s) in ChR2-expressing VTA dopamine neurons of TH–Cre mice while undergoing subthreshold exposure to social defeat (Fig. 1d). Mice that

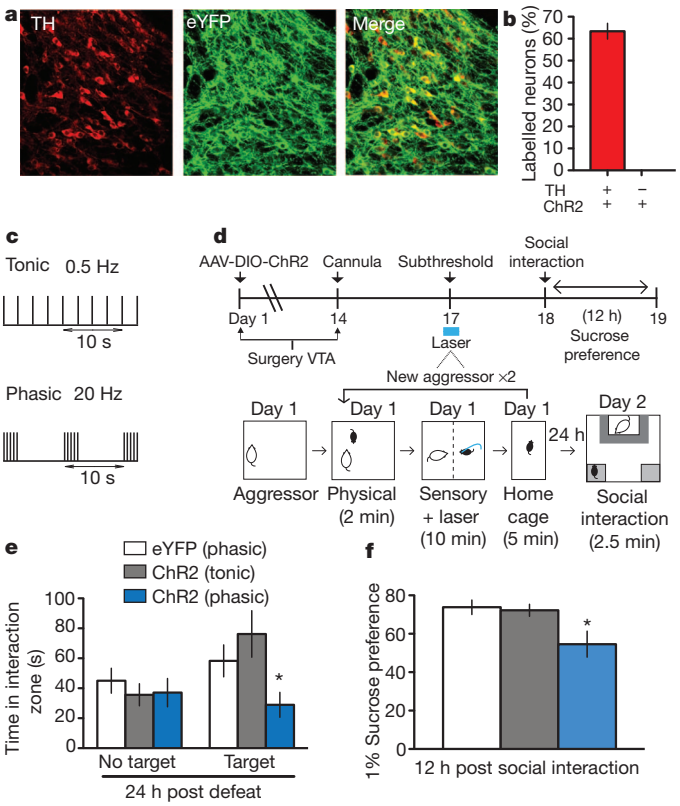

Figure 1 | Phasic, but not tonic, optical stimulation of VTA dopamine neurons during a subthreshold social defeat induces a susceptible phenotype. **a**, Confocal image showing co-expression of AAV-DIO-ChR2 in TH-positive dopamine cells from TH–Cre mice. **b**, Quantification shows that ChR2-expressing TH-positive cells are 62 ± 4% of total TH-positive neurons in the VTA. No expression of ChR2 was found in TH-negative neurons ($n = 2$–3 sections from $n = 4$ animals). **c**, Optical stimulation protocols for mimicking tonic (0.5-Hz) or phasic (20-Hz) firing. Note that for both stimulating protocols, 5 spikes are induced over each 10-s period. **d**, Top panel, experimental timeline. Bottom panel, detailed schematic of the subthreshold paradigm showing laser stimulation during social defeat. **e**, Social-interaction data from control, tonic and phasic groups. ($F_{2,30} = 4.70$, $P < 0.05$; post hoc test, $^*P < 0.05$; $n = 7$–14). **f**, Sucrose preference measured over a 12-h period after the social-interaction test ($F_{2,22} = 5.22$, $P < 0.05$; post hoc test, $^*P < 0.05$; $n = 7$–10). Error bars, ± s.e.m.

[1]Department of Pharmacology and Systems Therapeutics, Friedman Brain Institute, Mount Sinai School of Medicine, New York, New York 10029, USA. [2]Fishberg Department of Neuroscience, Friedman Brain Institute, Mount Sinai School of Medicine, New York, New York 10029, USA. [3]Departments of Bioengineering and Psychiatry and Behavioural Sciences, Stanford University, Stanford, California 94305, USA. [4]Laboratory of Molecular Genetics, Howard Hughes Medical Institute, Rockefeller University, New York, New York 10056, USA. [5]McGovern Institute for Brain Research, Massachusetts Institute of Technology, Cambridge, Massachusetts 02139, USA.
*These authors contributed equally to this work.

undergo this subthreshold paradigm do not exhibit social avoidance or other depression-like behaviours (Supplementary Fig. 1d), but they are more vulnerable to subsequent stress[5,15]. We stimulated VTA dopamine neurons during the subthreshold defeat paradigm and measured social interaction and sucrose preference as two sequelae of defeat stress: social avoidance and reduced sucrose preference characterize the susceptible phenotype induced by our repeated (10-day) social-defeat paradigm[5,8,10]. Mice that received phasic stimulation exhibited a robust increase in the depression-like phenotype as indicated by the significant decrease both in social interaction in the presence of a target mouse (Fig. 1e and Supplementary Fig. 1e–g) and in sucrose preference (Fig. 1f) compared to both tonic stimulated ChR2–eYFP mice and phasic stimulated eYFP control mice. These data confirm the functional importance of increased phasic, but not tonic, firing of VTA dopamine neurons during exposure to stress for promoting susceptibility for depression-like behavioural abnormalities.

To test directly the causal link between phasic dopamine-neuron firing and stress susceptibility, mice were exposed to subthreshold defeat and then to stimulation of VTA dopamine neurons during the social-interaction test (Supplementary Fig. 2a). Phasic stimulation of VTA dopamine neurons instantly induced a susceptible phenotype (increased social avoidance) during the social-interaction test in the presence of a target CD1 mouse (or a target C57 mouse, Supplementary Fig. 3), an effect not seen in tonic stimulated ChR2 mice or phasic stimulated eYFP control mice (Fig. 2a and Supplementary Fig. 2b–d). ChR2-expressing mice that received phasic stimulation during the brief 2.5-min social-interaction test also showed reduced sucrose preference compared to tonic-stimulated ChR2 mice or phasic-stimulated eYFP control mice (Fig. 2b). These findings are striking because they reveal the rapid induction of such depression-like behaviours that normally require repeated social-defeat stress.

In contrast to the ability of VTA dopamine-neuron stimulation to promote depression-like behaviours either during or after social-defeat stress, we found that phasic stimulation of these neurons in naive animals had no effect on social interaction, on sucrose preference or on baseline anxiety-related measures (Supplementary Fig. 4). These findings show that the pro-depression-like effects of VTA dopamine-neuron activation demonstrated here are context-specific, an important finding in light of the pro-reward consequences of such dopamine-neuron activation in other systems[6,7,9]. Furthermore, chronic mild stressors or physically aversive stimuli inhibit the activity of VTA dopamine neurons, whereas more severe stressors increase this activity[16,17], as is the case with severe social stress. Also, chronic mild stress and chronic social-defeat stress have been shown recently to produce different changes in extracellular levels of several neurotransmitters in a number of brain areas[18]. These findings raise the possibility that, in addition to context, the severity of stress is another important determinant of stress regulation of dopamine-neuron firing.

We next investigated whether phasic firing of VTA dopamine neurons could convert resilient mice to susceptible mice. Using our standard repeated (10-day) social-defeat paradigm[5,8,10], we identified the subgroup of mice that remained resilient based on normal social-interaction scores, which we know are highly correlated with normal sucrose preference and other behavioural and biochemical endpoints[5]. Our previous work had shown that VTA dopamine neurons of resilient mice display normal firing rates and patterns due to unique adaptations within these neurons that prevent the stress-induced increase in their excitability[5,8]. To test the effect of increased phasic stimulation of VTA dopamine neurons in resilient mice, we switched to herpes simplex virus (HSV)-ChR2 and control vectors with confirmed immunohistochemical and functional validation (Supplementary Fig. 5a–d).

HSV vectors have the advantage of expressing their transgenes very rapidly (within 24 h) compared to AAV vectors, which require 10–14 days for maximal expression[5,10,14]. In this experiment, wild-type mice were subjected to the standard repeated social-defeat stress and then a social-interaction test on day 11 to identify the resilient mice as noted above. Resilient mice were injected with HSV–eYFP or

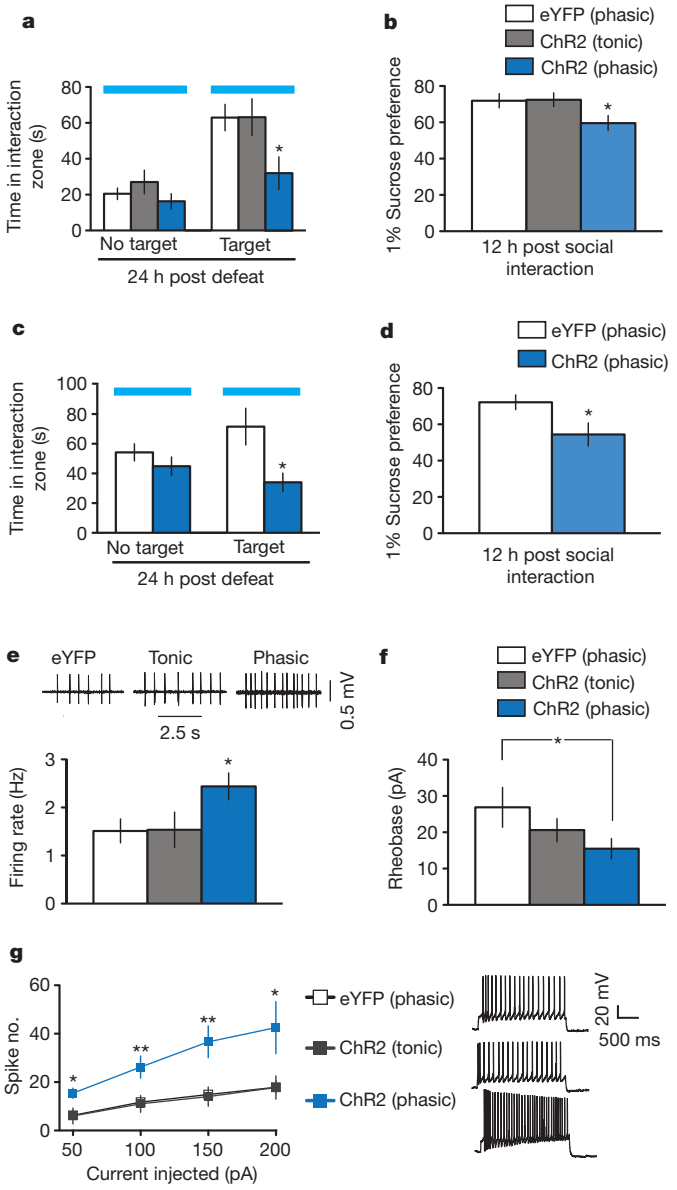

Figure 2 | Phasic optical stimulation of VTA dopamine neurons during the social-interaction test instantly induces a susceptible phenotype in two social-defeat paradigms. **a**, Social-interaction data in control, tonic and phasic groups ($F_{2,22} = 4.00$, $P < 0.05$; post hoc test, $^*P < 0.05$; $n = 7$–11). Blue light stimulation was used during the tests (blue horizontal bars in **a** and **c**). **b**, Sucrose preference measured over a 12-h period after the social-interaction test ($F_{2,25} = 3.47$, $P < 0.05$; post hoc test, $^*P < 0.05$; $n = 8$–11). **c**, Social-interaction data measured on day 17 ($t_{15} = 2.72$, $^*P < 0.05$; two-tailed *t*-test, $n = 11$–18). **d**, Sucrose preference measured over a 12-h period after the social-interaction test ($t_{17} = 2.34$, $^*P < 0.05$; two-tailed *t*-test, $n = 6$–12). **e**, Sample traces showing *in vitro* spontaneous activity of VTA dopamine neurons from TH–Cre mice that underwent tonic and phasic stimulation during the social-interaction test 24 h after subthreshold social defeat (see Supplementary Fig. 5j for the experimental timeline). Bar graph, comparison of spontaneous firing in VTA dopamine neurons from eYFP control, tonic and phasic-stimulated mice ($F_{2,50} = 3.19$, $P < 0.05$; post hoc test, $^*P < 0.05$; $n = 17$–19). **f**, Significantly less current was required to evoke a single spike in phasic-stimulated mice compared to eYFP control mice ($t_{21} = 1.8$, $^*P < 0.05$; one-tailed *t*-test, $n = 12$–16). **g**, VTA dopamine cells from phasic-stimulated mice display greater overall increased cell excitability in response to incrementally increased current injections (50, 100, 150 and 200 pA) than eYFP control and tonic-stimulated mice ($F_{2,140} = 16.13$, $P < 0.001$; post hoc test, $^*P < 0.05$ $^{**}P < 0.005$; $n = 5$–17). Error bars, ± s.e.m.

HSV-ChR2–eYFP and subsequently analysed in a second social-interaction test during which time they underwent optogenetic phasic stimulation (Supplementary Fig. 5e, f). Although optogenetically stimulated HSV–eYFP-injected mice remained resilient, optically induced phasic firing of the VTA of HSV-ChR2–eYFP injected mice instantly converted their behavioural phenotype from resilient to susceptible as evidenced by the decrease in time spent in the interaction zone (Fig. 2c and Supplementary Fig. 5g–i). Furthermore, such phasic firing of the VTA induced anhedonic traits as evidenced by decreased sucrose preference compared to HSV–eYFP-injected mice (Fig. 2d).

Given the striking impairment in sucrose preference approximately 12 h after the optogenetic activation of VTA neurons, we proposed that such stimulation might induce lasting changes in VTA dopamine-neuron excitability. To investigate this hypothesis, we measured intrinsic membrane properties of these neurons of TH–Cre mice that had previously undergone the subthreshold social-defeat paradigm followed by *in vivo* optogenetic stimulation during the social-interaction test (Supplementary Fig. 5j). Phasic stimulation induced increased VTA dopamine-neuronal excitability compared to eYFP and tonic-stimulated mice as measured by increased spontaneous (Fig. 2e) and evoked (Fig. 2f, g) activity 8–12 h after optical stimulation. These findings suggest that subthreshold defeat followed by acute optogenetic activation leads to long-lasting neuroadaptations in VTA dopamine neurons that underlie the sustained decrease in sucrose preference observed.

VTA dopamine neurons project broadly throughout the brain. The role of the VTA–NAc pathway in reward is well known[6,9,14], but it has also been implicated in stress responses, as has the VTA–mPFC pathway[1,2,4,5,10,19]. Therefore we were interested in investigating the role of these two distinct VTA projection pathways in promoting the susceptible and resilient phenotypes. We first investigated the VTA–NAc circuit by specifically labelling VTA neurons projecting to the NAc; this was accomplished by injecting the retrograde green fluorescent tracer lumafluor into the NAc and measuring the firing rate of dye-positive VTA–NAc neurons in control, susceptible and resilient mice after repeated (10-day) social-defeat stress (see Supplementary Fig. 6a, b for anatomical validation). We found that NAc-projecting VTA dopamine neurons in brain slices from susceptible mice showed a significantly higher firing rate compared to those of control and resilient mice (Fig. 3a, b), which is in agreement with increased phasic firing events from our previous work[5,8]. Next we used optogenetic techniques to selectively stimulate this VTA–NAc pathway. To do this, we injected a replication-defective version of the retrograde travelling pseudorabies virus expressing Cre (PRV–Cre) into the NAc and the Cre-dependent AAV-DIO-ChR2–eYFP into the VTA of wild-type mice (Supplementary Fig. 6c). Immunohistochemical and electrophysiological validation confirmed the viability of using PRV–Cre to express functional ChR2 in VTA cells projecting to the NAc (Supplementary Fig. 6d–h). Mice were then subjected to the subthreshold social-defeat paradigm and 24 h later were optogenetically stimulated during the social-interaction test (Supplementary 6i). Optical induction of phasic, but not tonic, firing in VTA–NAc neurons induced the susceptible phenotype as measured by increased social avoidance and decreased sucrose preference (Fig. 3c, d and Supplementary 6j, k). Although the vast majority of dopamine neurons in this pathway were optically stimulated, only a small number of non-dopamine neurons were labelled with our approaches. Further work will be needed to study any potential influence of these non-dopamine cells on stress responses.

To investigate the effect of inhibiting the VTA–NAc pathway on the expression of the stress response, we injected AAV-DIO-halorhodopsin (NpHR)–eYFP (version 3.0 of NpHR) into the VTA followed by PRV–Cre in the NAc (Supplementary Fig. 7a, b). Functional validation confirmed that yellow light (563 nm) reliably inhibited VTA neuronal firing both *in vitro* and *in vivo* (Supplementary Fig. 7c, d) and, importantly, we did not observe any NpHR-activated rebound effect in these neurons as a result of the light protocol that we used during the behavioural experiments (Supplementary Fig. 7e). Furthermore, anatomical quantification showed robust NpHR expression in VTA cells projecting to NAc (Supplementary Fig. 7f, g). Mice were first put through the standard repeated social-defeat stress paradigm followed by a social-interaction test on day 11 to identify the susceptible mice for eYFP control and NpHR groups (Supplementary Fig. 7h). Optogenetically stimulated DIO–eYFP injected mice remained susceptible in the second social-interaction test (both during target presence and absence), whereas inhibition of the VTA–NAc projection of DIO-NpHR–eYFP-injected mice instantly induced the resilient phenotype as evidenced by the increase in both the amount of time spent in the interaction zone and preference for sucrose (Fig. 3e, f and Supplementary Fig. 7i, j). These mice had undergone a chronic social-defeat paradigm and an earlier social-interaction test. It is therefore likely that the optogenetic attenuation of the increased activity of the VTA–NAc pathway that is typically seen in susceptible mice, combined with reactivation of the memory of the previous social-interaction test, resulted in those NpHR-injected mice spending longer times in the interaction zone, both in the absence and presence of a target mouse, during the second social-interaction test.

We also carried out experiments to investigate the functional importance of mPFC-projecting VTA dopamine neurons in promoting a susceptible phenotype (Fig. 4). We first labelled VTA neurons projecting to mPFC by injecting the retrograde red fluorescent tracer lumafluor into the mPFC (Supplementary Fig. 8a, b). Surprisingly, the firing rate of VTA–mPFC neurons was dramatically decreased in brain slices obtained from susceptible mice after repeated (10-day) social-defeat

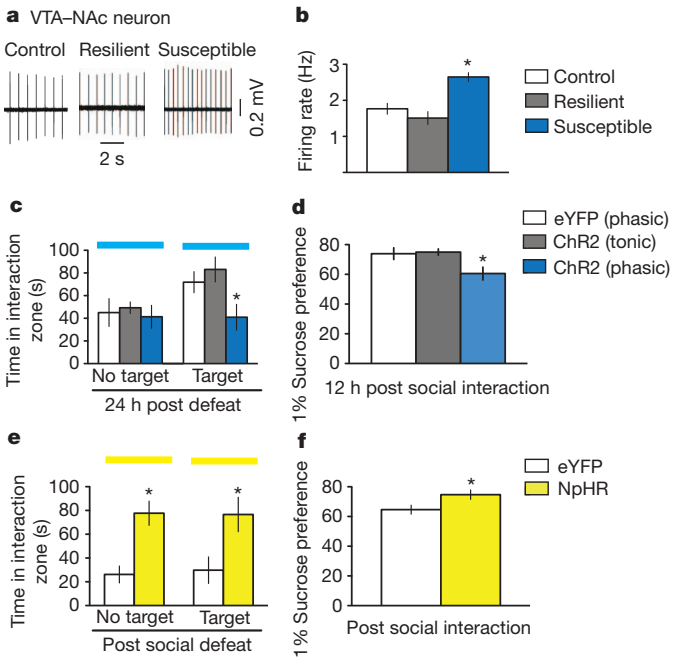

Figure 3 | Bidirectional effect of modulating the VTA–NAc pathway on susceptibility to social defeat. **a**, Sample traces recorded from VTA–NAc neurons in VTA slices. **b**, Firing rates of VTA–NAc neurons from control, resilient and susceptible mice ($F_{2,89} = 15.77$, $P < 0.001$; post hoc test, $^*P < 0.001$; $n = 12$–52). **c**, Social-interaction data obtained during optical stimulation of VTA–NAc neurons in control, tonic and phasic groups ($F_{2,20} = 4.43$, $P < 0.05$; post hoc test, $^*P < 0.05$; $n = 5$–10). Blue light stimulation was used during the tests (blue horizontal bars). **d**, Sucrose-preference data measured over a 12-h period after the social-interaction test ($F_{2,18} = 4.80$, $P < 0.05$; post hoc test, $^*P < 0.05$; $n = 5$–9). **e**, Social interaction during optical inhibition of VTA–NAc neurons in previously susceptible mice (No target: $t_{15} = 4.2$, $^*P < 0.001$; two-tailed t-test, $n = 8$–9; Target: $t_{15} = 2.6$, $^*P < 0.05$; two-tailed t-test, $n = 8$–9). Yellow light stimulation was used during the tests (yellow horizontal bars). **f**, Sucrose preference measured over a 12-h period after the social-interaction test ($t_{14} = 2.3$, $^*P < 0.05$; two-tailed t-test, $n = 8$–9). Error bars, ± s.e.m.

stress, compared to that of control and resilient mice (Fig. 4a, b). This is consistent with a recent report of decreased extracellular dopamine levels in this region after repeated social-defeat stress[18]. We next used optogenetic techniques to selectively stimulate the VTA–mPFC pathway. To do this, we injected the retrograde PRV–Cre viral vector into the mPFC and the Cre-dependent AAV-DIO-ChR2-eYFP into the VTA of wild-type mice (Supplementary Fig. 8c), and confirmed the viability of using PRV–Cre to express functional ChR2 in VTA cells projecting to mPFC (Supplementary Fig. 8d–h). Optically induced phasic firing of these VTA–mPFC neurons, during the social-interaction test in mice that had previously undergone subthreshold social defeat, had no effect on social interaction and sucrose preference, compared to tonic stimulation and control viral vectors (Fig. 4c, d and Supplementary Fig. 8i, j). We next investigated the effect of inhibiting the VTA–mPFC pathway on the expression of the stress response by injecting DIO-NpHR–eYFP into the VTA followed by PRV–Cre into the mPFC (Supplementary Fig. 9a–d). *In vivo* optical inhibition of the VTA–mPFC pathway by activation of NpHR, during the social-interaction test in mice that had previously undergone subthreshold social defeat, induced the susceptible phenotype as measured by decreased social interaction, an effect that is not seen in control mice (Fig. 4e and Supplementary Fig. 9e, f). Interestingly, there was no difference in sucrose preference (Fig. 4f).

Our study establishes a direct link between VTA dopamine-neuronal firing patterns and susceptibility to a depression-related phenotype, in cases in which phasic firing of NAc-projecting VTA dopamine neurons encodes a signal for susceptibility. This finding is consistent with the proposed role of VTA–NAc (mesolimbic) dopamine-neuronal phasic firing in this stress model: we previously showed that the VTA–NAc pathway is a key determinant of susceptibility versus resilience to repeated social-defeat stress[5], and that the pathophysiological increase in phasic firing occurs selectively in susceptible mice[8]. The observation that VTA dopamine-neuron phasic firing has a functional role in encoding for both depression-like symptoms after social-defeat stress, and conditioned place preference[7], suggests that firing patterns of these neurons and the subsequent encoding of the depressive or reward phenotype are highly context-dependent. Such encoding of stress versus reward is more complex still, because it is not only firing-pattern selective[7] but also dependent on the severity of stress (as noted above) and shows clear projection-pathway specificity[19].

In addition, our observation of the rapid onset of the susceptible phenotype in response to optical stimulation corresponds to the inferred function of mesolimbic dopamine neurons in mediating rapid antidepressant effects[1,20]. Similarly, hyperpolarization-activated cation channels (I_h), a key channel responsible for the transition from tonic to phasic firing of VTA dopamine neurons[21,22] that is highly expressed in VTA–NAc neurons[19], is increased in susceptible mice, whereas I_h inhibitors display rapid and long-lasting antidepressant-like efficacy[8,23]. Furthermore, the rapid antidepressant effects of ketamine[24–26], sleep deprivation[27] and deep brain stimulation[28–30] support the existence of rapidly reversible brain mechanisms and support the idea of regulating neural circuits to treat depression. Consistent with these studies, we show a rapid 'rescue' effect of VTA–NAc pathway inhibition when it occurs in the context of repeated severe social stress. In marked contrast, our findings that the VTA–mPFC pathway serves the opposite function to the VTA–NAc pathway, are consistent with a recent study demonstrating the differential role of largely distinct VTA dopamine neuron populations in response to rewarding versus aversive stimuli[19]. In addition, our observation that modulation of the VTA–NAc pathway but not the VTA–mPFC pathway induces anhedonic-like effects suggests a functional role for the VTA–NAc pathway but not VTA–mPFC pathway in encoding reward-related information in the context of depression. Our projection-specific findings thus provide new insights into the complex role that VTA dopamine neurons have in an individual's adaptations to repeated stress and the development of depression-like behavioural abnormalities.

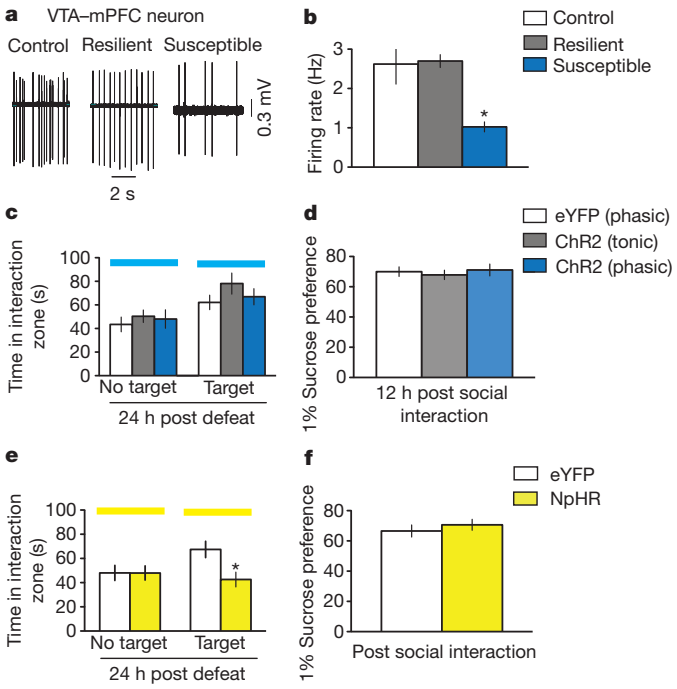

Figure 4 | Effect of modulating the VTA–mPFC pathway on susceptibility to social defeat. **a**, Sample traces recorded from VTA–mPFC neurons in VTA slices. **b**, Firing rates of VTA–mPFC neurons from control, resilient and susceptible mice ($F_{2,38} = 15.07$, $P = 0.0005$; post hoc test, $^*P < 0.005$; $n = 11$–15). **c**, Social-interaction data obtained by optical stimulation of VTA–mPFC neurons in control, tonic and phasic groups ($F_{2,39} = 1.29$, $P = 0.29$; $n = 11$–17). **d**, Sucrose-preference data measured over a 12-h period after the social-interaction test ($F_{2,33} = 0.19$, $P = 0.82$; $n = 10$–16). **e**, Social-interaction data obtained during optical inhibition of VTA–mPFC neurons ($t_{29} = 2.5$, $^*P < 0.05$; two-tailed t-test, $n = 12$–19). **f**, Sucrose preference measured over a 12-h period after the social-interaction test ($t_{29} = 0.38$, $P > 0.05$, $n = 12$–19). Error bars, ± s.e.m.

METHODS SUMMARY

Viral-vector delivery to discrete brain regions. Viral vectors (0.5 µl) were stereotaxically and bilaterally injected at a rate of 0.1 µl min^{-1}. AAV-DIO-ChR2–eYFP and AAV–eYFP (purchased from the University of North Carolina Vector Core Facility) were delivered into the VTA of TH–Cre mice. Retrograde PRV–Cre was injected into either NAc or mPFC and then AAV-DIO-ChR2–eYFP or AAV-DIO–eYFP was injected into the VTA. All viral vectors used were functionally validated with electrophysiological approaches in brain slices and/or intact animals. Retrograde pseudorabies virus (PRV)–Cre and PRV–GFP have a deletion in the viral thymidine kinase gene so that they do not replicate in non-dividing cells, cannot be transmitted trans-synaptically, and do not produce detectable effects on the health of infected neurons. Injected animals remained healthy when brain tissues were taken 7 to 10 days after surgery.

Social-defeat stress and social-interaction test. The subthreshold social-defeat paradigm involved placing the test C57BL/6J mouse into the home cage of a larger retired breeder mouse (CD1) for 2 min during which time the experimental mouse was physically attacked by the CD1 mouse. After two bouts of defeat the mouse was returned to its home cage. Mice underwent the social-interaction test 24 h after the defeat episodes. Mice received laser stimulation either during the subthreshold defeat encounters or during the subsequent social-interaction test. For some experiments in Figs 2 and 3, a repeated social-defeat paradigm (5–10 min defeat per day for 10 days) was used to separate out susceptible and resilient mice. The segregation of susceptible and resilient mice was based on the social-interaction test[5]. These subthreshold and repeated social-defeat paradigms have been extensively validated[5,8,10].

Light stimulation. For *in vivo* behavioural experiments using ChR2 mice (473 nm), these mice were given low-frequency tonic (0.5 Hz) or high-frequency phasic (20 Hz) light stimulations. In both tonic and phasic light-stimulation protocols, VTA dopamine neurons were exposed to 5 spikes over each 10-s period. For *in vivo* behavioural experiments using NpHR mice (563 nm), these mice were given 8 s light on and 2 s light off.

Full Methods and any associated references are available in the online version of the paper.

Received 1 March; accepted 25 October 2012.
Published online 12 December 2012.

1. Willner, P., Hale, A. S. & Argyropoulos, S. Dopaminergic mechanism of antidepressant action in depressed patients. *J. Affect. Disord.* **86,** 37–45 (2005).
2. Nestler, E. J. & Carlezon, W. A. Jr. The mesolimbic dopamine reward circuit in depression. *Biol. Psychiatry* **59,** 1151–1159 (2006).
3. Berton, O. & Nestler, E. J. New approaches to antidepressant drug discovery: beyond monoamines. *Nature Rev. Neurosci.* **7,** 137–151 (2006).
4. Yadid, G. & Friedman, A. Dynamics of the dopaminergic system as a key component to the understanding of depression. *Prog. Brain Res.* **172,** 265–286 (2008).
5. Krishnan, V. *et al.* Molecular adaptations underlying susceptibility and resistance to social defeat in brain reward regions. *Cell* **131,** 391–404 (2007).
6. Grace, A. A., Floresco, S. B., Goto, Y. & Lodge, D. J. Regulation of firing of dopaminergic neurons and control of goal-directed behaviors. *Trends Neurosci.* **30,** 220–227 (2007).
7. Tsai, H. C. *et al.* Phasic firing in dopaminergic neurons is sufficient for behavioral conditioning. *Science* **324,** 1080–1084 (2009).
8. Cao, J. L. *et al.* Mesolimbic dopamine neurons in the brain reward circuit mediate susceptibility to social defeat and antidepressant action. *J. Neurosci.* **30,** 16453–16458 (2010).
9. Schultz, W. Dopamine signals for reward value and risk: basic and recent data. *Behav. Brain Funct.* **6,** 24 (2010).
10. Berton, O. *et al.* Essential role of BDNF in the mesolimbic dopamine pathway in social defeat stress. *Science* **311,** 864–868 (2006).
11. Anstrom, K. K., Miczek, K. A. & Budygin, E. A. Increased phasic dopamine signaling in the mesolimbic pathway during social defeat in rats. *Neuroscience* **161,** 3–12 (2009).
12. Razzoli, M., Andreoli, M., Michielin, F., Quarta, D. & Sokal, D. M. Increased phasic activity of VTA dopamine neurons in mice 3 weeks after repeated social defeat. *Behav. Brain Res.* **218,** 253–257 (2011).
13. Krishnan, V., Berton, O. & Nestler, E. The use of animal models in psychiatric research and treatment. *Am. J. Psychiatry* **165,** 1109 (2008).
14. Lobo, M. K. *et al.* Cell type-specific loss of BDNF signaling mimics optogenetic control of cocaine reward. *Science* **330,** 385–390 (2010).
15. Iñiguez, S. D. *et al.* Extracellular signal-regulated kinase-2 within the ventral tegmental area regulates responses to stress. *J. Neurosci.* **30,** 7652–7663 (2010).
16. Valenti, O., Gill, K. M. & Grace, A. A. Different stressors produce excitation or inhibition of mesolimbic dopamine neuron activity: response alteration by stress pre-exposure. *Eur. J. Neurosci.* **35,** 1312–1321 (2012).
17. Ungless, M. A., Magill, P. J. & Bolam, J. P. Uniform inhibition of dopamine neurons in the ventral tegmental area by aversive stimuli. *Science* **303,** 2040–2042 (2004).
18. Venzala, E., Garcia-Garcia, A. L., Elizalde, N. & Tordera, R. M. Social vs. environmental stress models of depression from a behavioural and neurochemical approach. *Eur. Neuropsychopharmacol.* advance online publication, http://dx.doi.org/10.1016/j.euroneuro.2012.05.010 (June 27, 2012).
19. Lammel, S., Ion, D. I., Roeper, J. & Malenka, R. C. Projection-specific modulation of dopamine neuron synapses by aversive and rewarding stimuli. *Neuron* **70,** 855–862 (2011).
20. Willner, P. The mesolimbic dopamine system as a target for rapid antidepressant action. *Int. Clin. Psychopharmacol.* **12** (Suppl. 3), S7–S14 (1997).
21. Radulescu, A. R. Mechanisms explaining transitions between tonic and phasic firing in neuronal populations as predicted by a low dimensional firing rate model. *PLoS ONE* **5,** e12695 (2010).
22. Inyushin, M. U., Arencibia-Albite, F., Vazquez-Torres, R., Velez-Hernandez, M. E. & Jimenez-Rivera, C. A. Alpha-2 noradrenergic receptor activation inhibits the hyperpolarization-activated cation current (I_h) in neurons of the ventral tegmental area. *Neuroscience* **167,** 287–297 (2010).
23. Han, H. M. *et al.* Essential role of ventral tegmental area dopamine neurons in mediating the induction and rapid reversal of depression-like behaviours. Abstract, http://www.acnp.org/annualmeeting/programbooks.aspx (The 50th Anniversary Meeting of ACNP, 2011).
24. Berman, R. M. *et al.* Antidepressant effects of ketamine in depressed patients. *Biol. Psychiatry* **47,** 351–354 (2000).
25. Li, N. *et al.* mTOR-dependent synapse formation underlies the rapid antidepressant effects of NMDA antagonists. *Science* **329,** 959–964 (2010).
26. Autry, A. E. *et al.* NMDA receptor blockade at rest triggers rapid behavioural antidepressant responses. *Nature* **475,** 91–95 (2011).
27. Hemmeter, U. M., Hemmeter-Spernal, J. & Krieg, J. C. Sleep deprivation in depression. *Expert Rev. Neurother.* **10,** 1101–1115 (2010).
28. Giacobbe, P., Mayberg, H. S. & Lozano, A. M. Treatment resistant depression as a failure of brain homeostatic mechanisms: implications for deep brain stimulation. *Exp. Neurol.* **219,** 44–52 (2009).
29. Sartorius, A. *et al.* Remission of major depression under deep brain stimulation of the lateral habenula in a therapy-refractory patient. *Biol. Psychiatry* **67,** e9–e11 (2010).
30. Li, B. *et al.* Synaptic potentiation onto habenula neurons in the learned helplessness model of depression. *Nature* **470,** 535–539 (2011).

Supplementary Information is available in the online version of the paper.

Acknowledgements This work was supported by the National Institute of Mental Health (R01 MH092306 to D.C. and M.H.H.), Johnson & Johnson IMHRO Rising Star Translational Research Award (M.H.H.), the National Research Service Awards (F31 MH095425 to J.J.W. and F32 MH096464 to A.K.F) and the Mount Sinai PREP R25 GM064118 (B.J.). We would like to thank K. Roy for help with some of the schematics in the figures, and we thank R. Cachope and J. Cheer for help with chronic fibre implantation techniques.

Author Contributions D.C., J.J.W., A.K.F., B.J., J.W.K., D.F., D.J.C., H.C.T., M.K.L., M.S.M.-R. and S.M.K. collected and analysed data. L.P., A.R.N. M.E., A.D., E.M., R.L.N., S.J.R., J.M.F., K.D. and E.J.N. generated and provided viral vectors and TH–Cre mice. D.C., J.J.W., E.J.N. and M.H.H. designed and wrote the paper.

Author Information Reprints and permissions information is available at www.nature.com/reprints. The authors declare no competing financial interests. Readers are welcome to comment on the online version of the paper. Correspondence and requests for materials should be addressed to M.H.H. (ming-hu.han@mssm.edu).

METHODS

Experimental subjects. CD1 male retired breeders (Charles River), C57BL/6J male mice (7–9 weeks; Jackson Laboratories) and tyrosine hydroxylase (TH)–Cre male transgenic mice (7-9 weeks; Charles Rivers) were used in these studies. TH–Cre transgenic mice (EM:00254) were obtained from the European Mutant Archive and mated with C57BL/7 wild-type mice[7,31]. All TH–Cre subjects used in this study were backcrossed for at least 10 generations. Mice were singly housed and maintained on a 12-h light–dark cycle with food and water available *ad libitum*. All animal protocols were in accordance with the National Institutes of Health Guide for Care and Use of Laboratory Animals and approved by the Mount Sinai Institutional Animal Care and Use Committee.

Virus vectors. AAV-DIO-ChR2–eYFP, AAV-DIO-NpHR–eYFP and AAV-DIO–eYFP virus plasmids[32] were initially generated using previous protocols[33] and then purchased from the University of North Carolina vector core facility (UNC). HSV-ChR2–eYFP and HSV–eYFP were provided by the laboratory of R.L.N. (MIT). Retrograde pseudorabies virus (PRV)–Cre was engineered by the laboratory of J.M.F. (Rockefeller University).

Stereotaxic surgery, viral mediated gene transfer, cannula placement and optic-fibre placement. Mice were anaesthetized with a ketamine (100 mg kg^{-1}) and xylaxine (10 mg kg^{-1}) mixture, placed in a stereotaxic apparatus (Kopf Instruments) and their skull was exposed by scalpel incision. For ChR2 viruses, 33-gauge needles were placed either bilaterally or unilaterally at a 0° angle into the VTA (anterior–posterior, −3.3 mm; lateral–medial, +0.5 mm; dorsal–ventral, −4.4 mm) and 0.5–1 µl of virus was infused at a rate of 0.1 µl min^{-1}. NpHR virus was injected bilaterally into the VTA at a 7° angle (anterior–posterior, −3.3 mm; lateral–medial, +1.05 mm; dorsal–ventral, −4.6 mm) and 1 µl of virus was infused at a rate of 0.1 µl min^{-1}. For PRV–Cre viral injections 33-gauge needles were placed bilaterally at either a 10° angle into the NAc (anterior–posterior, +1.6 mm; lateral–medial, +1.5 mm; dorsal–ventral, −4.4 mm) or 15° angle into the mPFC (anterior–posterior, +1.7; lateral–medial, +0.75; dorsal–ventral, −2.5) and 0.5–1 µl of virus was infused at a rate of 0.1 µl min^{-1}. Bilateral (26-gauge) or unilateral (20-gauge) cannulae, with a length of 3.9 mm from the cannula base, were implanted over the VTA (anterior–posterior, −3.3 mm; lateral–medial, +0.5 mm; dorsal–ventral, −3.7 mm). For secure fixture of the cannula to the skull, instant adhesive (Loctite 454) was placed between the base of the cannula and the skull, and then dental cement (Ortho-Jet) was added around the cannula and the skull. For NpHR-expressing viral vectors, we used the chronically implantable optical-fibre system[34]. Chronically implantable fibres were homemade with 200 µm core optic fibre and were implanted into the VTA at a 7° angle (anterior–posterior, −3.3 mm; lateral–medial, +1.05 mm; dorsal–ventral, −4.4 mm). For secure fixture of the implantable fibre to the skull, the skull was dried and then industrial-strength dental cement (Grip cement; Dentsply) was added between the base of the implantable fibre and the skull. For AAV surgeries on TH–Cre mice (cell-specific study), we carried out two surgeries in which we first injected the ChR2 virus then performed cannula surgery at least 2 weeks later when the AAV virus was expressed. Mice were allowed to recover for at least 3 days before starting the behavioural paradigm. For AAV surgeries on C57 mice (projection-specific study) we again undertook two surgeries, in which ChR2 virus surgery was carried out and then PRV–Cre and cannula or implantable-fibre surgery was carried out at least 2 weeks later. To enable the mice to recover and for PRV–Cre to retrograde back to the VTA we waited 5 days before starting the behavioural paradigm. For HSV surgeries both ChR2 virus and cannula placement were carried out on the same day and mice were allowed to recover for at least 3 days before starting the behavioural paradigm. Lumafluor tracing for retrograde labelling of VTA neurons projecting to NAc or mPFC, the retrobeads were injected into the NAc or mPFC at the coordinates mentioned previously. Lumafluor (1 µl) was injected into each hemisphere.

For *in vivo* optical control of VTA neuronal firing with ChR2 experiments, a 200-µm core optic fibre was modified for attachment to the cannula. When the fibre was secured to the cannula, the tip of the fibre extended approximately 0.5 mm beyond the cannula. This experimental set up was based on and slightly modified from previous studies[14,35]. For NpHR experiments 200 µm fibre core was attached to an chronically implanted fibre. Optic fibres were only secured *in vivo* during the behavioural paradigm (during subthreshold social-defeat or social-interaction tests).

Blue light stimulation. Optical fibres (Thor Labs, BFL37-200) were connected using an FC/PC adaptor to a 473-nm blue laser diode (Crystal Laser, BCL-473-050-M), and a stimulator (Agilent Technologies, no. 33220A) was used to generate blue light pulses. For *in vitro* slice electrophysiological validation of ChR2 activation we tested 0.1–50-Hz stimulation protocols. For *in vivo* optrode recordings we tested similar stimulation protocols. For all *in vivo* behavioural experiments, mice were given either low-frequency tonic (0.5 Hz, 15 ms) or high-frequency phasic (20 Hz, 40 ms) light stimulations. In both tonic and phasic light stimulation protocols, VTA dopamine neurons were exposed to 5 spikes over each 10-s period (Fig. 1c). For ChR2 activation during the subthreshold social defeat, mice received bilateral stimulation, whereas for all ChR2 activation during the social-interaction test mice received unilateral stimulations.

Yellow light stimulation. Optical fibres (Thor Labs, SFS200/220Y) were connected using an FC/PC adaptor to a 561-nm yellow laser diode (Crystal Laser, CL561-050-L), and a stimulator (Agilent Technologies, no. 33220A) was used to generate yellow light pulses. For *in vitro* slice electrophysiological validation of NpHR activation, we tested different durations of yellow light activation (1–60 s duration) to examine the duration-dependent inhibition of the firing rate (Supplementary Fig. 7d). For all *in vivo* behavioural experiments, mice was given a protocol of 8 s of yellow light on and then by 2 s light off during the social-interaction test. All NpHR experiments were performed using bilateral stimulations.

Social-defeat stress and social interaction. Mice underwent either a subthreshold social-defeat stress paradigm or a repeated social-defeat stress paradigm[36]. The subthreshold paradigm involved placing the test mice (intruder) into the home cage of a larger, retired 'resident' breeder mouse (CD1) for 2 min during which time the experimental mouse was physically attacked (defeated) by the CD1 mouse. After 2 min of physical interaction, the experimental mice underwent 10 min of sensory stress. For this, a perforated plexiglass partition was placed in the middle of the CD1 mouse home cage, and the resident CD1 and intruder experimental mouse were physically separated but kept next to each other. After 10 min of sensory stress the experimental mouse was returned to its home cage for 5 min after which time it went through a second round of physical interaction and sensory stress in the home cage of a new CD1 mouse. After two bouts of defeats the experimental mouse was returned to its home cage and underwent social-interaction test the next day. In a subset of experiments the experimental mice underwent bilateral light stimulation (5 min per hemisphere), in order to stimulate VTA dopamine cells, during the sensory-stress period.

For the repeated social-defeat paradigm, an experimental mouse was placed into the home cage of a CD1 mouse for 10 min during which time it was physically defeated by the CD1 mouse. After 1 min of physical interaction, the CD1 and experimental mouse were maintained in sensory contact for 24 h using a perforated plexiglass partition dividing the resident home cage in two. The experimental mice were exposed to a new CD1 mouse home cage for 10 consecutive days and tested for social interaction on day 11. Both subthreshold and repeated social defeat were carried out between 13:00 and 15:00.

Social-avoidance behaviour towards a novel CD1 mouse was measured in a two-stage social-interaction test. In the first 2.5-min test (target absent), the experimental mouse was allowed to freely explore a square-shaped arena (44 × 44 cm) containing a wire mesh cage (10 × 6 cm) placed on one side of the arena. In the second 2.5 min test, the experimental mouse was reintroduced back into the arena with an unfamiliar CD1 mouse contained behind a wire mesh cage. Video tracking software (Ethovision 3.0, Noldus) was used to measure the amount of time the experimental mouse spent in the 'interaction zone' (14 × 26 cm), 'corner zone' (10 × 10 cm) and 'total travel' within the arena. In a subset of studies experimental mice underwent unilateral blue light stimulation to activate the VTA dopamine cells or yellow light stimulation to inhibit VTA dopamine cells, during both the target absent and target present sessions of the social-interaction test. The interaction ratio was measured as (interaction time, target present)/(interaction time, target absent) and normalized to 100. Susceptible and resilient mice were segregated based on the interaction ratio: mice with scores <100 were defined as 'susceptible' and those with scores ≥ 100 were defined as 'resilient'. To confirm that the optogenetic activation-induced depression-related avoidance is not a simple fear memory of a CD1 aggressor, a social-interaction test using a C57 mouse as a target was carried out. Mice that had undergone subthreshold social defeat and then phasic stimulation during the social-interaction test similarly avoided the non-aggressive C57 social target to the same degree as observed with a CD1 target (Supplementary Fig. 2). This is consistent with our previous work showing that a C57 social target induced social avoidance in the repeated social-defeat paradigm[5].

Sucrose preference. Mice were initially habituated to 50-ml tubes with stoppers fitted with ball-point sipper tubes (a two-bottle choice) filled with drinking water 2 days before the sucrose-preference measurements. After completion of the social-interaction test mice were given access to a two-bottle choice of water or 1% sucrose solution. Bottles containing water and sucrose were weighed at several time points during the day at 15:00, 18:00 and 09:00 for 3 days. The position of the bottles was interchanged (left to right, right to left) after each weight measurement to ensure that the mice did not develop a side preference. Sucrose preference was calculated as a percentage (amount of sucrose consumed × 100 (bottle A)/total volume consumed (bottles A + B)). Total sucrose consumption during the first 12 h after the social-interaction test was measured and used to obtain sucrose preference in this study.

Elevated plus maze. Mice were placed in the centre of an elevated plus maze (arms are 33 × 5 cm, with 25-cm tall walls on the closed arms) and their behaviour was

digitally tracked for 5 min. Mice received VTA optical stimulation during the whole duration of the elevated plus maze. A video-tracking system (Ethovision 3.0, Noldus) was used to measure the amount of time spent in the closed and open arms.

Open field. Mice were tested for their activity during 15 min in an open field arena (44 × 44 cm). A video-tracking system (Ethovision 3.0, Noldus) was used to measure the locomotor activity of the animal, as well as the time spent in the centre (34 × 34 cm) and periphery of the test arena.

***In vitro* patch-clamp electrophysiology.** Whole-cell optogenetic recordings were obtained from VTA dopamine neurons in acute brain slices from TH–Cre mice that had been stereotaxically injected with AAV-DIO-ChR2–eYFP into the VTA, C57 mice that been injected with HSV-ChR2–eYFP into the VTA or C57 mice that been injected with the retrograde viral vector PRV–Cre in either the NAc or mPFc, and AAV-DIO–ChR2–eYFP or AAV-DIO-NpHR–eYFP into the VTA. Cell-attached recordings were obtained from VTA dopamine neurons in acute brain slices from wild type C57 mice that had been stereotaxically injected with the retrograde dye lumafluor in either NAc or mPFc. To minimize stress and to obtain healthy VTA slices, mice were anaesthetized and perfused immediately for 40–60 s with ice-cold aCSF (artificial cerebrospinal fluid), which contained 128 mM NaCl, 3 mM KCl, 1.25 mM NaH_2PO4, 10 mM D-glucose, 24 mM $NaHCO_3$, 2 mM $CaCl_2$ and 2 mM $MgCl_2$ (oxygenated with 95% O_2 and 5% CO_2, pH 7.4, 295–305 mOsm). Acute brain slices containing VTA dopamine neurons were cut using a microslicer (DTK-1000, Ted Pella) in cold sucrose aCSF, which was derived by fully replacing NaCl with 254 mM sucrose and saturated by 95% O_2 and 5% CO_2. Slices were maintained in holding chambers with aCSF for 1 h at 37 °C. Patch pipettes (3–5 mΩ) for whole-cell current-clamp, voltage-clamp and cell-attached recordings were filled with internal solution containing the following: 115 mM potassium gluconate, 20 mM KCl, 1.5 mM $MgCl_2$, 10 mM phosphocreatine, 10 mM HEPES, 2 mM magnesium ATP and 0.5 mM GTP (pH 7.2, 285 mOsm). Whole-cell and cell-attached recordings were carried out using aCSF at 34 °C (flow rate = 2.5 ml min^{-1}). For whole-cell recordings during optogenetic stimulation resting membrane potential and action potentials were recorded in current-clamp mode and inward current measurements were made in voltage-clamp mode using the Multiclamp 700B amplifier and data acquisition was done in pClamp 10 (Molecular Devices). Series resistance was monitored during the experiments and membrane currents and voltages were filtered at 3 kHz (Bessel filter). For ChR2 experiments, sustained and trains (0.1–50 Hz) of blue light were generated by a stimulator (mentioned above) and delivered to VTA dopamine neurons expressing ChR2 through a 200-mm optic fibre attached to a 473-nm laser. For NpHR experiments, different durations of yellow light were generated by a stimulator mentioned above and delivered to VTA dopamine neurons expressing NpHR through a 200-mm optic fibre attached to a 561-nm laser. For cell-attached action potential recordings, signals were band-pass filtered at 300 Hz–1 kHz to identify dopamine neurons and were then bessel filtered at 10 kHz (gain 50) using a Multiclamp 700B amplifier and data acquisition was carried out using pClamp 10. For measurements of the spontaneous activity of VTA dopamine neurons, cell-attached recordings were performed. To measure the intrinsic membrane properties of VTA dopamine neurons, whole-cell recordings were carried out in current-clamp mode and spikes were induced by incremental increases of current injection (each step increase was 50 pA; range 50–200 pA).

***In vivo* optrode recording.** Viral injection and *in vivo* optrode recordings were carried out as described previously[7,37]. AAV-DIO-ChR2–eYFP was injected into VTA (anterior–posterior, −3.44 mm; lateral–medial, +0.48 mm; dorsal–ventral, −4.4 mm) of TH–Cre mice and left for at least 2 weeks to allow for viral expression. Prior to recordings mice were deeply anaesthetized with a ketamine and xylaxine mixture, and placed on a stereotactic frame and attached to a temperature regulator. The area of skull directly above the VTA was removed and an optrode consisting of a tungsten electrode (1 mΩ resistance; 125 μm length) tightly bundled with an optical fibre (200-μm core, 0.2 NA) was lowered to the boundary of the VTA (anterior–posterior, −3.44 mm; lateral–medial, +0.48 mm; dorsal–ventral, −4 mm). The tip of the electrode protruded about 0.4 mm beyond the optical fibre to ensure illumination of the recorded neurons. At the VTA boundary simultaneous optical stimulation and recordings of the electrical response of neurons expressing ChR2 was carried out as the optrodes were gradually lowered in 0.1-mm increments until a clear response to optical stimulation was measured. The optical fibre was coupled to a 473-nm solid-state laser diode with an approximately 20-mW output. Recorded signals were band-pass filtered at 300 Hz–5 kHz using an 1800 Microelectrode AC amplifier.

Immunohistochemistry. For double-immunofluorescence experiments, tissue sections were fixed in 4% (weight divided by volume; wt/vol) PBS-buffered paraformaldehyde. Tissues and cells were blocked in PBS-T (0.3% Triton X-100) including 2% (wt/vol) bovine serum albumin (BSA; Sigma) and then exposed overnight to these primary antibody mixtures: anti-GFP (Invitrogen, 1:2000) and anti-TH (Sigma, 1:10,000). Detection of primary antibodies was carried out with mixtures of the secondary antibodies Cy2-anti-mouse and Cy3-conjugated anti-rabbit (1:500; Jackson ImmunoResearch). Anti-NeuN (Aves Laboratories, NUN) raised from chicken was used at a dilution ratio of 1:1000 and was detected by Cy3-anti-chicken. For TH labelling, anti-TH (Sigma) from mouse at a dilution ratio of 1:5000 was used and detected with Cy5-anti-mouse. For GFP labelling, anti-GFP (Invitrogen) from rabbit was used at a dilution ratio of 1:2000 and was detected by Cy2-anti-rabbit. Tissues and cells were counterstained and mounted with anti-fade solution, including 4′,6-diamidino-2-phenylindole (DAPI; VectaShield, Vector Laboratories). Sections were subsequently imaged (×20 magnification) on a LSM 710 confocal (Zeiss). Cell counting was carried out manually using ImageJ. For immuno-validation of PRV–Cre, animals were killed with a lethal dose of Isofluorane and then transcardially perfused with PBS then 10% formalin 5–10 days post PRV–Cre injections. After perfusion, brains were kept in 10% formalin at 4 °C for 18–24 h, at which point the brains were transferred to PBS and sliced into coronal sections using a vibrating blade microtome (Leica Microsystems, model VT1000S). For immunostaining, we processed the slices using antibodies against GFP (Abcam, chicken, 1:1000) and tyrosine hydroxylase (Pel-Freez, rabbit, 1:1000). The antibodies were labelled with goat anti-chicken Alexa 488 and goat anti-rabbit Alexa 633 (Invitrogen, 1:1000), respectively. mCherry expression from the AAV was sufficiently intense for confocal microscopy. Sections were imaged at ×20 magnification for analysis, which was performed manually.

31. Lindeberg, J. *et al.* Transgenic expression of Cre recombinase from the tyrosine hydroxylase locus. *Genesis* **40,** 67–73 (2004).
32. Cardin, J. A. *et al.* Targeted optogenetic stimulation and recording of neurons in vivo using cell-type-specific expression of Channelrhodopsin-2. *Nature Protocols* **5,** 247–254 (2010).
33. Hommel, J. D., Sears, R. M., Georgescu, D., Simmons, D. L. & DiLeone, R. J. Local gene knockdown in the brain using viral-mediated RNA interference. *Nature Med.* **9,** 1539–1544 (2003).
34. Sparta, D. R. *et al.* Construction of implantable optical fibers for long-term optogenetic manipulation of neural circuits. *Nature Protocols* **7,** 12–23 (2011).
35. Gradinaru, V. *et al.* Targeting and readout strategies for fast optical neural control *in vitro* and *in vivo*. *J. Neurosci.* **27,** 14231–14238 (2007).
36. Golden, S. A., Covington, H. E. III, Berton, O. & Russo, S. J. A standardized protocol for repeated social defeat stress in mice. *Nature Protocols* **6,** 1183–1191 (2011).
37. Stuber, G. D. *et al.* Excitatory transmission from the amygdala to nucleus accumbens facilitates reward seeking. *Nature* **475,** 377–380 (2011).